A Low-Cost C-band Active Reflector for InSAR deformation monitoring

Guido Luzi [1], Pedro F. Espín-López [1], Qi Gao [1], Marta Monfort [2], Pavel Pavlovsky [2], Michele Crosetto [1]

[1] Centre Tecnològic de Telecomunicacions de Catalunya - CERCA (CTTC-CERCA), Geomatics Research Unit, Av. Gauss 7, E-08860 Castelldefels, Barcelona, Spain – (gluzi, pespin, qgao, mcrosetto@cttc.cat)
[2] GeoKinesia, Gran Via de Carlos III, 98, 10, 08028, Barcelona, Spain (marta.monfort, pavel.pavlovsky@geokinesia.com)

Keywords: InSAR**,** Active reflector, Deformation.

Abstract

InSAR often demands the installation of artificial reflectors, usually represented by Passive Corner Reflectors (PCR). This occurs when in the imaged areas the coherence is low, and the density of Persistent Scatterers (PS) is scarce or even non-existent. For missions based on C-band sensor as Sentinel-1, PCRs capable of providing a high phase accuracy are cumbersome, and heavy, and the installation is difficult and costly. For this reason, the use of Active Reflectors (AR), compact and smaller with respect to PCRs, can be a valid alternative especially in mountain vegetated or snow-covered areas, or glaciers. The use of these devices has not yet largely spread due to their high sensitivity over long interval to annual/seasonal temperature range of variation which reduces their reliability. This work focuses on the analysis of the performance of a C band low-cost AR tested in a real field campaign based on the interferometric processing of Sentinel-1 images aimed at monitoring a forested slope, located in Andorra, partially collapsed some years ago. Phase stability is investigated using data acquired during an experimental campaign carried out in where also several PCRs have been installed. The experimental tests confirm that the device is capable to provide a millimetric accuracy over a significant temporal interval and can be used as reference point for a network of PCR installed in instable areas.

1. Introduction

A widespread approach of the last decades for ground deformation detection and monitoring is the DInSAR (Differential Interferometric Synthetic Aperture Radar) technique, which is based on SAR images acquired from orbiting satellites. This technique is based on the processing of large stacks of SAR images, acquired at different times, according to the revisit time of the spaceborne radar. The accuracy of the measurements is influenced by several factors as the main characteristics of the sensor such as wavelength, radar quality of the images, number of images analysed, and the type of the measured targets. Examples of “good points”, i.e. which maintain along the time a statistical correlation sufficient to provide reliable phase information, are man-made objects, e.g. buildings and infrastructures, but also natural features such as rock surfaces. Persistent Scatterer Interferometry (PSI), one of the most used DInSAR processing technique, makes use of large stacks of SAR images, demanding that the coherence of the targets to be monitored maintains sufficiently high over the entire observation period; the effectiveness of this approach demands a high density of points with low DA (Dispersion of Amplitude), a statistical parameter of the amplitude response of the target (Ferretti et al., 2001). This is usually guaranteed in urban, peri-urban and industrial areas while in mountain forested and snow-covered areas such points can be totally missing. In these last cases, the installation of artificial reflectors is necessary. The most used solution is the installation of target with a simple geometrical shape, designed to perform a high radar reflectivity, i.e. a strong response to the SAR microwaves, namely Passive Corner Reflectors (PCR) (Xia et al., 2002). To provide a high radar reflectivity and accordingly high accuracy in phase measurement (Garthwaite, 2017), they must be considerably larger than the radar wavelength, and in C-band the necessary actual dimensions, make them heavy and difficult to deploy; furthermore, they can have mechanical stability problems in areas characterized by strong wind. For example, considering the most used PCR, the metal triangular trihedral, the requested size of the target for a sub-millimetre accuracy is not smaller than 1.7 m (Garthwaite, 2017).

Active Reflectors (ARs), which are basically a device which receives the radar signal and re-transmits an amplified version of the same to the satellite (Brunfeldt, 1984, Mahapatra et al. 2014, Meister et al., 2022), can substitute the use of PCRs. They are usually smaller, lighter and easy to deploy. Their main limitation is they require a power source, which is typically provided by a battery and a solar panel, and that their phase stability can be affected by a high sensitivity over long interval to annual/seasonal temperature range of variation which reduces their reliability, and in term of deformations the achievable stability is not about a few millimetres (Czikharddt et al., 2021; Meister et al., 2024).

This paper reports the DInSAR spaceborne based monitoring of a rockslide, probably induced by roadside excavations, in a mountain area where the dense vegetation demanded the installation of artificial reflectors to achieve some representative points where estimate the deformation. Eight PCRs, aluminium square-based trihedral reflectors, have been installed on the slope above the rockslide detachment crown, to monitor the behaviour after the stabilization works in different locations covering the monitored area, approximatively 25000 m^2. In addition, an AR, a prototype developed at CTTC and accurately tested in controlled environment (Luzi et al., 2021), was installed in a stable area. The estimate of the deformation in the moving area is retrieved through the interferometric processing of a set on Sentinel-1 images acquired along more than three years. Deformation is estimated in correspondence to the PCR location and using as reference the AR phase measured in a stable area. Although the AR response showed a certain instability due to seasonal variations of air humidity and temperature, a satisfactory millimetre accuracy has been achieved. These results are one of the main outcomes of the

European research project MOMPA (Monitoring of Ground Movements and Action Protocol), whose objective is to provide useful tools for the prevention and management of risks due to slope movements, based on the satellite monitoring InSAR (Interferometric SAR) technique, exploiting medium-resolution Sentinel-1, one of the sensors of the spaceborne ESA missions supporting Copernicus program.

2. Materials and Methods

2.1 The Satellite imagery processing

The SAR image set used in this work consists of 137 images from December 4, 2020 to May 5 2024. They are Sentinel-1 SLC images, descending pass, relative orbit number: 110, polarization: VV. A total amount of 521 interferograms with maximum temporal baseline of 30 days were processed using CTTC Persistent Scatterer Interferometry (PSI) processing chain (Devanthery et al. 2014). The Digital Elevation Model (DEM) generated by the Shuttle Topographic Mission (SRTM) with 30 m resolution was used. For the interferometric processing IW mode acquisitions have been processed.

In Figure 1 we show an amplitude image where the different reflectors distributed along the area geographically identified by the latitude and longitude of the vertex of the rectangle; details about them are given in the next paragraph. Both PCR and AR are processed as standard PSs. The intensity of the AR response, as expected from theoretical calculation and laboratory test on the AR, is largely higher than the that of PCR whose size is sub-optimal.

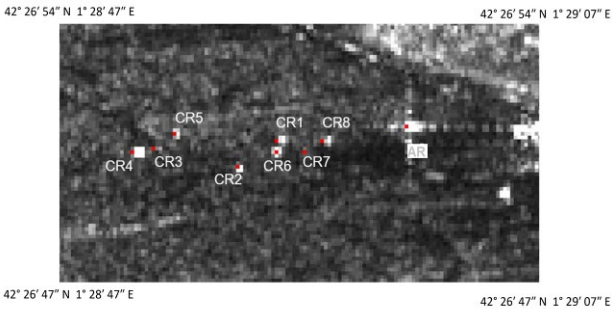

Figure 1. Mean amplitude image obtained averaging 60 SLC S1 images. CR: Passive Corner reflectors, AR: Active Reflector.

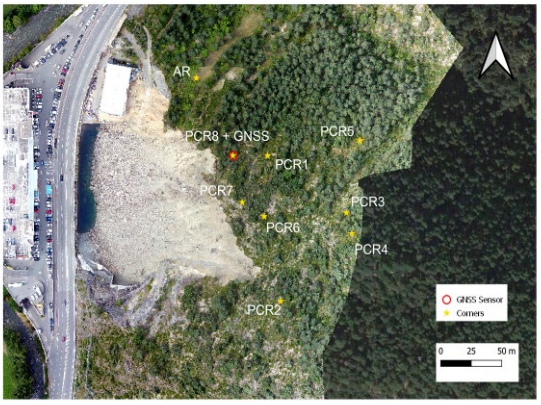

Figure 2. Map of collapsed area and the locations of the different artificial reflectors.

2.2 The Artificial Reflectors

The network of seven PCRs of the same size, inner edge length of 0.65 m, are made of aluminium and their geometrical shape the shape is a square-based trihedral with trimmed faces. The calculated maximum RCS (Czikhardt et al. 2021) of 33.4 dBm2 at C band, can theoretically provide a millimetre accuracy, according to the Signal To Clutter (SCR) ratio available in the area. The AR is designed to work with the Copernicus Sentinel-1A and Sentinel-1B sensors and it operates at 5.405 GHz ± 50 MHz. The design and implementation of this ARs has been carefully made with the goal of a producing a low-cost system, with low power consumption, portable and installable with fast and simple procedures. Figure 2 shows a map of the monitored area with indicated the location of the installed reflectors. The markers indicate the different available benchmarks. The orientations of AR and PCRs are: Azimuth 100° (Nord) for both; elevation: 16° for the PCR, to take into account the direction of peak RCS, which makes a grazing angle of approximately 35° with any of the side plates, and 51º for the AR. In Figure 3 we show an example of the AR response in the Sentinel-1 SAR images available in the EO Browser (https://apps.sentinel-hub.com/eo-browser/). The relatively high brightness confirms how the target outstands from the radar clutter with its typical sync behaviour in each intensity image.

In the following Figures 4 and 5 we show respectively the backscattering coefficient calculated from GRD data (Miranda et al. 2007) in the case of one PCR (#4) and the AR. In this plot, as expected, the PCR shows a lower mean value of backscattering with respect to the AR. In its temporal series shown in Figure 4 we also observe an outstanding minimum, in winter 2021, probably due to the presence of snow or other unknown factors reducing its radar response. On the other hand, in the AR temporal series there are two periods when it did not work due to powering problems; in one case the reason was that the battery discharged completely for insufficient solar powering (January 2022), while in the second case it was due to a cable fault (September 2021). The substitution of the battery with another with higher capacity fixed the issue: the AR has been working till today without any break since May 2022. Of note also the similar intensity of the clutter (radar noise in the observed area in absence of outstanding targets), a bit higher to -15 dB in both cases; this can be seen from Figures 4 and 5 when the targets were not yet installed, before December 2020, or in the two malfunctioning periods of the AR.

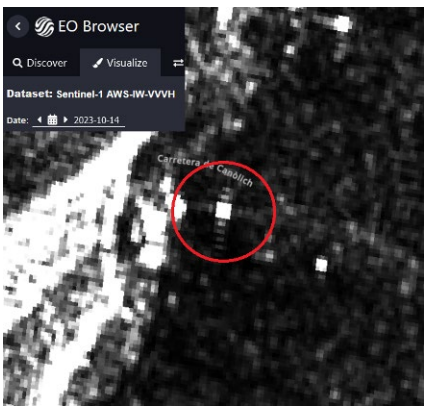

Figure 3. Example of an intensity map of the monitored area corresponding to the Sentinel-1 acquisition (VV) of 14 October 2023 with enhanced (red circle) the response of the AR; image downloaded from https://sentinel.esa.int/documents/2.

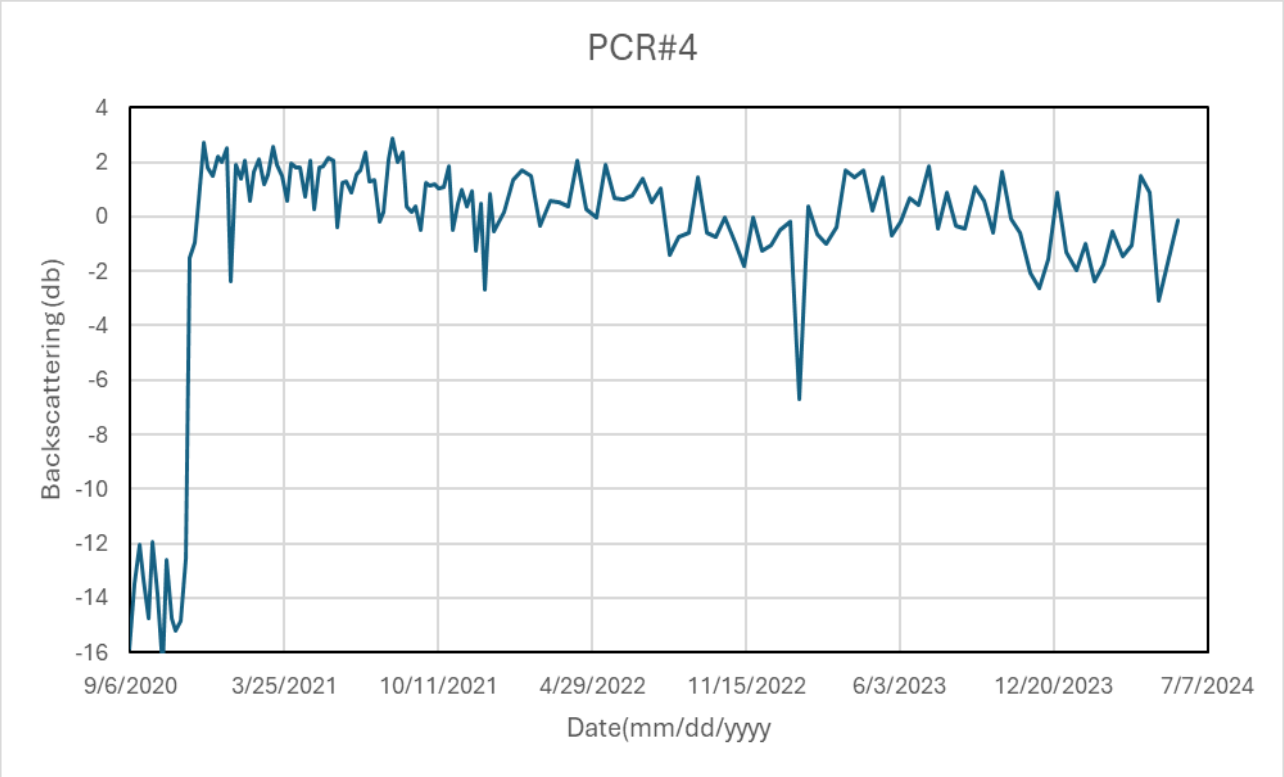

Figure 4. Backscattering coefficient of PCR#4 measured along the observed period (September 2020-May 2024).

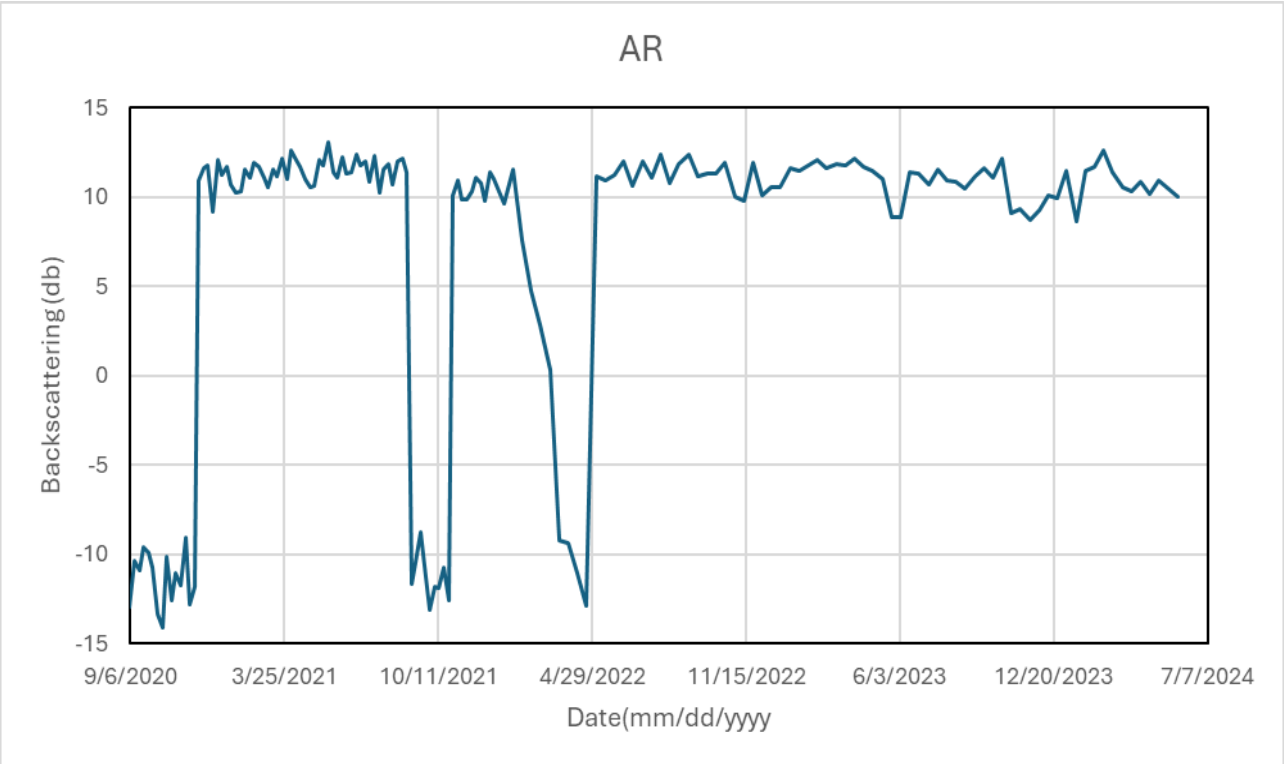

Figure 5. Backscattering coefficient of the AR measured along the observed period (September 2020-May 2024).

3. Results

The processing of the interferometric phase obtained from the complex SLC Radar data allows to estimate the temporal series of the AR displacement. We must consider that the effect of the seasonal thermal variations of the AR electronic device’s temperature can introduces a fluctuating phase affecting the measurement of the differential phase at different times. This additional term must be corrected when it is not negligible with respect to the deformation term associated to the mechanical deformation of the area objective of the monitoring. Although reference ground truth is missing, a geological stability analysis of the observed area states that the area where the AR is installed is stable. To carry out this analysis, we first observe, shown in Figure 6, the temporal series of the phase variation retrieved from the AR response, considered as virtual displacement corresponding to the instability of the device.

Mean Value	Standard Deviation	Mean Square Error
-0.57	1.86	3.7

Table 1. Statistical parameters of the data shown in Figure 6.

The variation of the virtual displacement maintains between ±5 although it seems to slightly increase in the last period. The linear regression calculation does not show a significant correlation, a yearly periodic trend can be figure out. Table 1 reports the main parameters calculated over the entire period. A standard deviation of 1.86 mm and the low offset of 0.57 mm represent a fair result considering that in landslide monitoring an accuracy of a few millimetres over three years can be considered valuable for operative use.

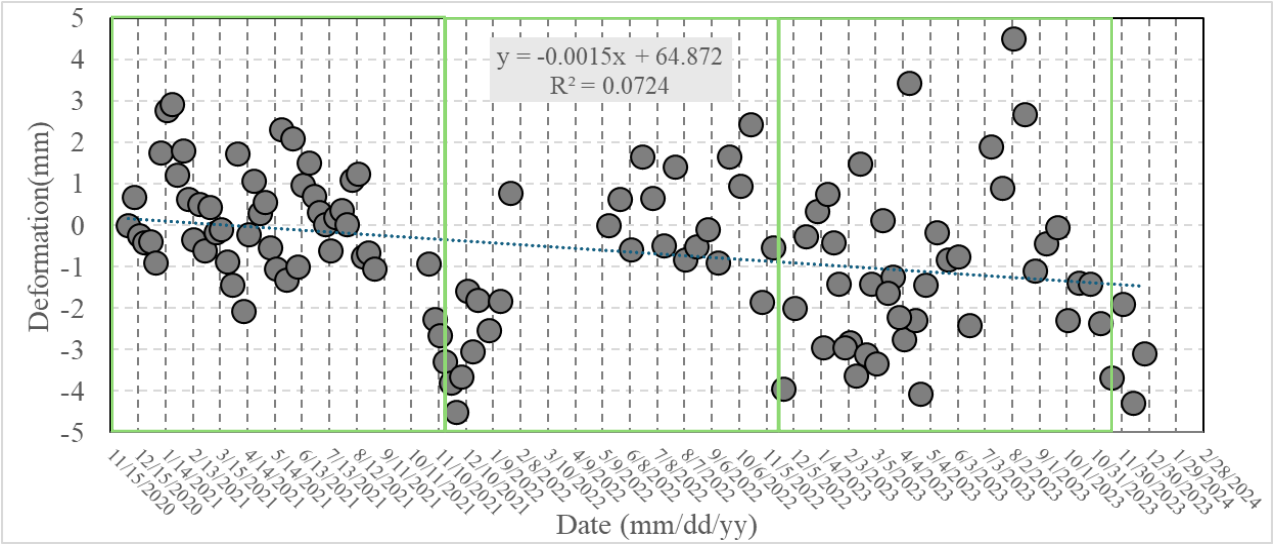

Figure 6. Deformation retrieved from interferometric processing of the phase data acquired from November 202 to February 2024. In correspondence of the AR: green rectangles mark a one-year period.

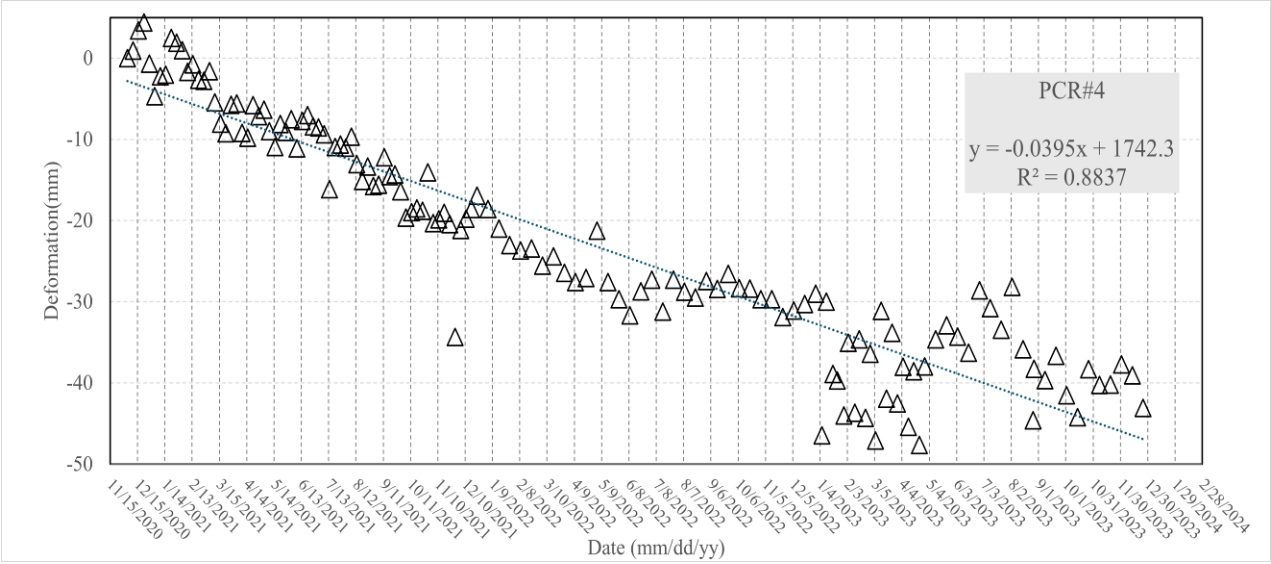

Figure 7. Deformation retrieved from interferometric processing of the phase data acquired from November 202 to February 2024 correspondence of the PCR #4.

In Figure 7 we show the displacement measured through the PCR #4, which is the one who maintained the more stable and higher amplitude signal (see Figure 4). The PCR are installed in a dense vegetated area and subject to mountain weather events as wind, rain and snow falls. These factors can affect the mechanical stability and the radar response of the target, and the relative stability and intensity of their response can be considered a quality factor when data are analysed over long temporal periods. In this case the target is installed in an area where the deformation is acting. Observing the plot, although the data of the last period appear more instable, a linear trend, correlation coefficient R=0.94, can be estimated. The slope corresponds to a mean rate of about 2 cm per year. Anyway, the phase retrieved for the PCRs is obtained taking as reference the phase of the AR, installed in a stable area, and for this reason the more instable signal of the AR in the last period (see Figure 6) introduces an instability also in the PCR response.

4. Conclusions

In this paper, the deformation of a slope recently affected by a collapse is monitored using DInSAR and temporal series of SAR images coming from Sentinel-1 mission. The absence of natural permanent scatterers was partially fixed using a network of passive reflectors and one active reflector.

The active device has been installed in a stable area and its phase has been used as reference point for the retrieval of the passive targets. Results show that the active reflector, although suffering from a significant variation due to seasonal periodical changes in air temperature and humidity, can provide a stability of the order of a few millimetres along three years of the experimental period.

Acknowledgements

This work has been partially funded by AGAUR, Generalitat de Catalunya, through the Consolidated Research Group RSE, “Geomatics” (Ref: 2021-SGR-00536). This work is part of the Spanish Grant SARAI, PID2020-116540RB-C21, funded by MCIN/AEI/ 10.13039/501100011033.

References

Brunfeldt, D.R.; Ulaby, F.T., 1984. Active reflector for radar calibration. *IEEE Transactions on Geoscience and Remote Sensing*, GE-22, 165–169.

Chengfan, L., Jingyuan, Y., Zhao, J., Zhang, G., Shan, X., 2012. The selection of artificial corner reflectors based on RCS analysis. *Acta Geophys.*, 60, 43–58, doi:10.2478/s11600-011-0060-y.

Luzi, G., Barra, A., Gao, Q., F. Espín-López, P., Palamà, R., Monserrat, O., Colell, X., 2022. A low-cost active reflector and a passive corner reflector network for assisting landslide monitoring using multi-temporal InSAR. *Remote Sensing Letters*, 13(11), 1080-1089.

Crosetto, M.; Monserrat, O.; Cuevas-González, M.; Devanthéry, N.; Crippa, B. Persistent scatterer interferometry: A review. ISPRS J. Photogramm. Remote Sens. 2016, 115, 78–89.

Czikhardt R., H. van der Marel, F.J. van Leijen and R.F. Hanssen, 2022. Estimating Signal-to-Clutter Ratio of InSAR Corner Reflectors From SAR Time Series. *IEEE Geoscience and Remote Sensing Letters*, vol. 19, pp. 1-5, 2022.

Czikhardt, R., van der Marel, H., Papco, J., Hanssen, R.F., 2021. On the Efficacy of Compact Radar Transponders for InSAR Geodesy: Results of Multi-year Field Tests. *IEEE Transactions on Geoscience and Remote Sensing*, 9570285.

Devanthéry, N., Crosetto, M., Monserrat, O., Cuevas-González, M., Crippa, B., 2014. An Approach to Persistent Scatterer Interferometry. *Remote Sensing*, *6*, 6662-6679.

Doerry, A.W., Brock, B.C., 2009. Radar Cross Section of Triangular Trihedral Reflector with Extended Bottom Plate 2009; SAND2009-2993; Sandia National Laboratories: Albuquerque, NM, USA.

Ferretti, A., Prati, C., Rocca, F., 2001. Permanent scatterers in SAR interferometry. *IEEE Transactions on Geoscience and Remote Sensing*, vol. 39, no.1, pp.8-20, DOI: 10.1109/36.898661

Garthwaite M., 2017. On the Design of Radar Corner Reflectors for Deformation Monitoring in Multi-Frequency InSAR. *Remote. Sensing* 9, 648, 2017, doi:10.3390/rs9070648.

Hounam, D.; Zwick, H.; Rabus, B., 2008. A permanent response SAR transponder for monitoring ground targets and features. Proceedings of the 7th European Conference on Synthetic Aperture Radar, Friedrichshafen, Germany, 2–5 June 2008; pp. 1–4.

Jauvin, M., Yan, Y., Trouvé, E., Fruneau, B., Gay, M., Girard, B., 2019. Integration of Corner Reflectors for the Monitoring of Mountain Glacier Areas with Sentinel-1 Time Series. *Remote Sens.* 2019, 11, 988, doi:10.3390/rs11080988.

Komac, M., Holley, R., Mahapatra, P., van der Marel, H., Bavec, M., 2015. Coupling of GPS/GNSS and radar interferometric data for a 3D surface displacement monitoring of landslides. *Landslides*, 12, 241–257, doi:10.1007/s10346-014-0482-0.

Luzi, G., Espín-López, P.F., Mira Pérez, F., Monserrat, O., Crosetto, M., 2021. A Low-Cost Active Reflector for Interferometric Monitoring Based on Sentinel-1 SAR Images. *Sensors*, 21, 2008. https://doi.org/10.3390/s21062008

Mahapatra, P.S., Samiei-Esfahany, S., van der Marel, H., Hanssen, R.F., 2014. On the use of transponders as coherent radar targets for SAR interferometry. *IEEE Transactions on Geoscience and Remote Sensing*, 52, 1869–1878, doi:10.1109/TGRS.2013.2255881.

Marinkovic P., G. Ketelaar, F. van Leijen, R. Hanssen, 2007. InSAR quality control—analysis of five years of corner reflector time series. Proceedings of the 5th International Workshop on ERS/Envisat SAR Interferometry (FRINGE '07), Frascati, Italy, November 2007.

Meister, A., Balasis-Levinsen, J., Keller, K., Pedersen, M. R. V., Merryman Boncori, J. P. and Jensen, M., 2024. A field test of compact active transponders for InSAR geodesy. *Journal of Geodetic Science*, vol. 14, no. 1, pp. 20220164. https://doi.org/10.1515/jogs-2022-0164.

Miranda, N., Meadows, P. J., Type, D., Note, T., 2015. Radiometric calibration of S-1 level-1 products generated by the

S-1 IPF. https://sentinel. esa. int/documents/247904/685163/S1-Radiometric-Calibration-V1. 0. pdf.

Parker, A., Featherstone W., Penna N., Filmer, M., Garthwaite, M.C., 2017. Practical Considerations before Installing Ground-Based Geodetic Infrastructure for Integrated InSAR and cGNSS Monitoring of Vertical Land Motion. *Sensors*, 17, 1753, doi:10.3390/s17081753 2017.

Qin, Y., Perissin, D. Lei, L., 2013. The design and experiments on corner reflectors for urban ground deformation monitoring in Hong Kong. *International Journal of Antennas and Propagation*, 2013.

Quin, G., Loreaux, P., 2013. Submillimeter Accuracy of Multipass Corner Reflector Monitoring by PS Technique. *IEEE Transactions on Geoscience and Remote Sensing*, 51, 1775–1783, doi:10.1109/TGRS.2012.2206600

Sarabandi, K., Oh, Y., Ulaby, F.T., 1992. Performance characterization of polarimetric active radar calibrators and a new single antenna design. *IEEE Transactions on Antennas and Propagation*, 1992, 40, 1147–1154, doi:10.1109/8.182446.

Xia Y., H. Kaufmann, and G. Xiaofang, 2002. Differential SAR interferometry using corner reflectors. *IEEE Proceedings of IGARSS 2002*, Toronto (CD-ROM) (2002).